



Research article

Unveiling the link between inflammasomes and skin cutaneous melanoma: Insights into expression patterns and immunotherapy response prediction

Yu Sheng¹, Jing Liu¹, Miao Zhang² and Shuyun Zheng^{1,*}

¹ Department of Dermatology, The First Affiliated Hospital of Harbin Medical University, Heilongjiang 150001, China

² Department of Dermatology, Heilongjiang Provincial Hospital, Heilongjiang 150036, China

* **Correspondence:** Email: zheng@hrbmu.edu.cn.

Abstract: Skin cutaneous melanoma (SKCM) is one of the most malignant forms of skin cancer, characterized by its high metastatic potential and low cure rate in advanced stages. Despite advancements in clinical therapies, the overall cure rate for SKCM remains low due to its resistance to conventional treatments. Inflammation is associated with the activation and regulation of inflammatory responses and plays a crucial role in the immune system. It has been implicated in various physiological and pathological processes, including cancer. However, the mechanisms of inflammasome activation in SKCM remain largely unexplored. In this study, we quantified the expression level of six inflammasome-related gene sets using transcriptomic data from SKCM patients. As a result, we found that inflammasome features were closely associated with various clinical characteristics and served as a favorable prognostic factor for patients. A functional enrichment analysis revealed the oncogenic role of inflammasome features in SKCM. Unsupervised clustering was applied to identify immune clusters and inflammatory subtypes, revealing a significant overlap between immune cluster 4 and SKCM subtype 2. The CASP1, GSDMD, NLRP3, IL1B, and IL18 features could predict immune checkpoint blockade therapy response in various SKCM cohorts. In conclusion, our study highlighted the significant association between the inflammasome and cancer treatment. Understanding the role of inflammasome signaling in SKCM pathology can help identify potential therapeutic targets and improve patient prognosis.

Keywords: skin cutaneous melanoma; inflammasome; prognosis; tumor immune microenvironment; immunotherapy

1. Introduction

Skin cutaneous melanoma (SKCM) is one of the most aggressive skin cancers, which has become a significant public health problem [1,2]. Its highly metastatic and invasive nature has led to a poor patient prognosis [3]. Despite significant advancements in clinical treatment approaches, including targeted therapies and immunotherapy, SKCM remains a severe clinical challenge [4]. Therefore, understanding the molecular mechanisms of SKCM is crucial for the effective prevention and improvement of patient prognosis [5].

Inflammation is a vital physiological response of the immune system, playing an essential role in both immune regulation and cancer [6]. The inflammasome, which is a multiprotein complex, serves as a critical mediator in the inflammatory process [7]. It is involved in various biological processes, including immune responses and cancer development [8]. Aberrant inflammasome activation can contribute to tumor development, progression, and metastasis [9,10]. NLRP3, CASP1, GSDMD, IL1B, and IL18 are interconnected components of inflammasome signaling, working together to regulate the inflammatory response [11]. Upon activation, NLRP3 recruits CASP1 and cleaves GSDMD, releasing IL1B and IL18 [12,13]. In turn, IL1B can promote the expression of NLRP3 and CASP1, thereby establishing a positive feedback loop in the inflammatory signaling cascade [14–16]. This intricate interplay between inflammation features highlights their coordinated involvement in mediating inflammation and suggests their potential as therapeutic targets for cancer [8]. Despite the recognized importance of inflammasome in cancer, there is a lack of comprehensive characterization of the inflammasome complex in SKCM.

Immune checkpoint blockade (ICB) therapy has become a breakthrough in cancer treatments, which involves targeting key regulatory checkpoints, including PD-1/PD-L1 and CTLA-4, to restore and enhance anti-tumor immune responses [17,18]. ICB therapy has demonstrated remarkable efficacy across multiple malignancies, including SKCM [19,20]. ICB therapy has revolutionized treatment options for SKCM patients, leading to durable clinical benefits and an improved overall survival in patients [21]. Despite the remarkable achievements of ICB therapy, the emergence of immune resistance poses a significant challenge to its effectiveness [22–24]. Therefore, there is a pressing need to elucidate the mechanisms underlying ICB therapy resistance. The inflammasome complex represents an intriguing target for immune checkpoint therapy [25,26]. Modulating the inflammasome pathway has the potential to augment antitumor immune responses and enhance the effectiveness of immune checkpoint inhibitors [27]. Exploring the interplay between inflammasome activation and ICB in melanoma could provide valuable insights into novel therapeutic strategies and improve patient outcomes.

In this study, we quantified the expression level of six inflammasome features, including CASP1, GSDMD, NLRP3, IL1B, IL18, and inflammasome complexes (IC) features, based on transcriptomic data, to comprehensively characterize the role of inflammasome features in tumorigenesis and progression. These inflammasome features exhibited a strong correlation with clinical characteristics. They were all dysregulated and served oncogenic roles in SKCM samples. The unsupervised clustering method identified four immune clusters and two SKCM subtypes, and significant overlaps were found between immune clusters and SKCM subtypes. Lastly, inflammasome features were implicated in the ICB immunotherapy response. In conclusion, our study highlighted the significant role of inflammasomes in SKCM, shedding light on their potential implications for SKCM progression, therapeutic strategies, and survival outcomes of patients. Furthermore, investigating the interplay between inflammasomes and ICB resistance is crucial for unraveling the underlying mechanisms in SKCM treatment.

2. Materials and methods

2.1. Collection of inflammasome-related gene sets

Six gene sets representing distinct inflammasome features were collected from previous studies: 1) 30 NLRP3-related genes [28]; 2) 15 IC-related genes [14]; 3) 34 CASP1-related genes [29] 4) 72 IL1B-related genes [14]; 5) 8 IL18-related genes [30]; and 6) 13 GSDMD-related genes [30]. Each gene set represents different steps of inflammasome signaling.

2.2. Acquisition of gene expression profile and clinical information

Fragments Per Kilobase of transcript per Million mapped reads upper quartile (FPKM-UQ) of RNA-seq data from the Cancer Genome Atlas data portal (TCGA) of SKCM patients and non-cancerous tissues from the Genotype-Tissue Expression (GTEx) consortium [31] were downloaded from the University of California, Santa Cruz (UCSC) Xena platform [32] (<https://xenabrowser.net/>). Approximately 19,724 protein-coding genes were obtained. Expression profile was log-transformed for analysis. Clinical patient information, including age, gender, TNM staging, Clark level, and cancer type (metastatic/primary), were obtained from UCSC Xena.

2.3. Identification of dysregulated inflammasome features and genes

A single-sample gene-set enrichment analysis (ssGSEA) was used to quantify the expression level of each inflammasome feature across various samples. We applied the R “limma” v3.54.2 package [33] to identify dysregulated inflammasome features and protein-coding genes. Features with a Benjamini-Hochberg (BH) adjusted p-value < 0.01 were defined as dysregulated; genes with a BH adjusted p-value < 0.01 and fold change > 2 were defined as dysregulated.

2.4. Tumor immune microenvironment (TIME) of SKCM

The tumor purity, stromal and immune cell abundances describing the TIME of SKCM were inferred by the Estimation of Stromal and Immune Cells in Malignant Tumours using Expression data (ESTIMATE) [34]. Four TIME classifications defined by 29 transcriptomic-based gene expression signatures, including angiogenesis fibrosis, anti-tumor microenvironment, malignant cell properties, and pro-tumor microenvironment, were obtained from a previous study [35]. A ssGSEA was used to quantify the enrichment level of each TIME signature. Distinct immune subtypes of SKCM patients were identified by an unsupervised hierarchical clustering method.

2.5. Inflammasome feature-defined SKCM patient subtypes

The R ‘Consensus ClusterPlus’ v1.62.0 package was applied to perform unsupervised consensus clustering on SKCM samples [36]. The clustering procedure using the inflammasome features matrix was repeated 5,000 times, thereby subsampling 80% of the samples. The optimal number of clusters was determined by the relative change in the area under the cumulative distribution function (CDF) curves and the Calinski criterion.

2.6. Survival analysis

Patients' overall survival (OS) and progression-free survival (PFS) information were downloaded for the USCS Xena platform. The R "survival" v3.5.5 and "survminer" v0.4.9 packages were applied to conduct uni and multi-variate Cox proportional hazards regression models. Inflammasome features with a Cox p-value < 0.05 were defined as significant. A hazard ratio (HR) < 1 was defined as a protective feature, while an HR > 1 was defined as a risky feature. Then, Kaplan-Meier curves were utilized to compare the survival status of different groups. A log-rank p-value < 0.05 was identified as a prognosis-related feature. A nomogram was constructed by the R "rms" v6.6.0 package and evaluated by a calibration plot.

2.7. Functional enrichment analysis

Gene ontology (GO), Kyoto Encyclopedia of Genes and Genomes (KEGG) pathway, and Reactome gene sets enrichment were conducted by the Metascape platform (<https://metascape.org/>) [37]. Ten oncogenic signaling pathways were obtained from a previous study [38]. Cancer hallmark gene sets were obtained from a previous study [39]. GO Biological Process (BP) and functional pathway gene sets were downloaded from MSigDB [40,41] (<https://www.gsea-msigdb.org/gsea/msigdb>). The R "fgsea" v1.24.0 package was applied to conduct a Gene Set Enrichment Analysis (GSEA).

2.8. Prediction of ICB therapy response

Three cohorts of SKCM patients who received ICB therapy were collected from previous studies [42,43] (Table 1). Patients who either partially or completely responded (P/CR) to ICB therapy were considered as responders, while patients with either a stable disease (SD) or progressive disease (PD) status were considered as non-responders. The R "pROC" v1.18.0 package was used to calculate the area under the curve (AUCs) of the receiver operating characteristic (ROC) curve for discriminating responders vs non-responders. Then, we used the R "e1071" v1.7.13 package to train the support vector machines (SVM) classifier based on the Gide cohort to predict the response of TCGA SKCM patients.

Table 1. Datasets used for ICB response analysis.

Cohort	Treatment	Patients	R	NR	PMID
Gide et al. [42]	anti-PD-1	41	19	22	30753825
Gide et al. [42]	anti-CTLA-4 + PD-1	51	35	16	30753825
GSE91061	anti-CTLA-4 + PD-1	105	23	82	29033130

2.9. Statistical analysis

A Mann-Whitney U test was used to compare the ssGSEA level in different groups. The Kruskal-Wallis test was used to compare ssGSEA levels among multiple groups. Spearman's correlation test was used to perform a correlation analysis. A P-value < 0.05 was considered as statistically significant. The statistical analysis in this study was performed by the R 4.2.3 software.

3. Results

3.1. Clinical relevance of inflammasome features in SKCM

The overall workflow of this study is displayed in Figure S1. To quantify the expression level of six inflammasome features, ssGSEA was performed on TCGA and GTEx samples. A differential expression analysis showed that CASP1, GSDMD, and NLRP3 features were upregulated in cancer samples, while IL18, IL1B, and IC features were downregulated in cancer samples (Figure 1(A), Figure S2(A)). Next, we investigated the associations between the clinical characteristics and the inflammasome features. Results showed that the expression level of the CASP1, GSDMD, NLRP3, and IC features decreased with the progression of the T stage (Figure 1(B) and (C), Figure S2(B) and (C)).

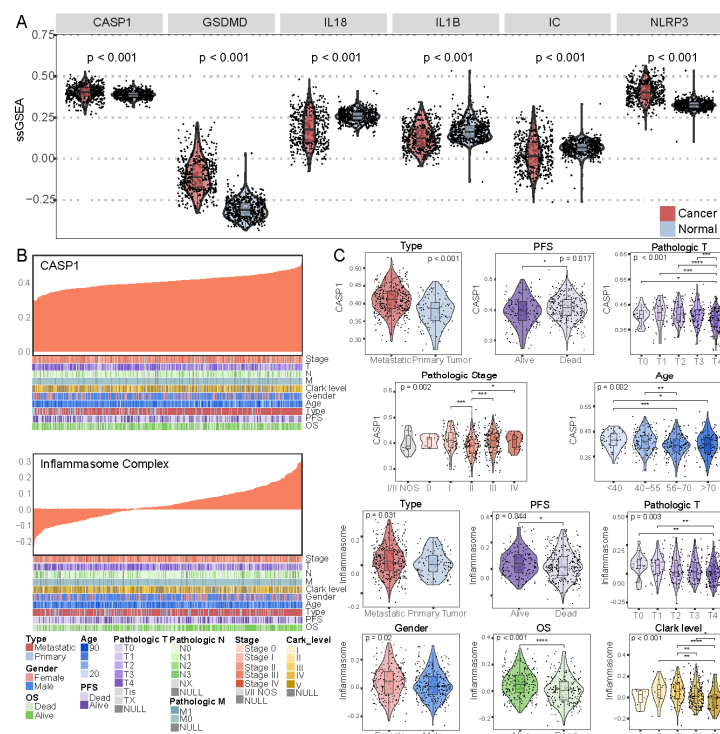


Figure 1. Correlations between inflammasome features and clinical characteristics in SKCM. (A) The violin plot illustrates the expression levels of inflammasome features in SKCM and normal samples. (B) The correlations between inflammasome feature levels and clinical characteristics, with samples sorted in ascending order based on inflammasome expression levels. (C) The violin plot illustrates the differences in the expression levels of inflammasome features among different groups of clinical characteristics.

These four features were upregulated in the metastatic samples compared to the primary tumor samples. The CASP1, GSDMD, NLRP3, and IL1B features demonstrated significant differences across pathological stages. Regarding the Clark level, we found that the GSDMD, NLRP3, and IC features first increased and then decreased with the progression of the Clark level. As for any gender differences, the GSDMD, IL1B, and IC features exhibited higher expression levels in female samples compared to male samples. The only age-related difference was found in the CASP1 feature, whose expression level decreased with age. No significant differences were found in the M and N stages. Patients with different

survival statuses exhibited significant differences in the levels of inflammasome features, whether OS or PFS. In conclusion, the expression levels of the inflammasome features were significantly associated with various clinical characteristics of SKCM.

3.2. Inflammasome features served as favorable factors for patient prognosis

To explore the associations between patient prognosis and the expression level of inflammasome features, we performed a survival analysis on TCGA SKCM patients. As shown in the K-M curves, patients with high expression of the CASP1, GSDMD, NLRP3, IL1B, and IC features exhibited improved prognoses (Figure 2(A)). The univariate Cox regression model results showed that these five features could serve as favorable factors for the patients' OS (Figure S3). Only the IL1B and IC features were associated with the patients' PFS. Next, we performed a multivariate Cox regression model to identify independent prognostic factors. Among the six inflammasome features, only the CASP1 and IC features remained significantly associated with overall survival (Figure 2(B)). Therefore, we constructed a nomogram based on these two independent prognostic factors and the age of patients. The nomogram was used to predict three- and five-year survival probabilities and the median survival time of SKCM patients (Figure 2(C)). Then, we used a calibration plot to assess the predictive accuracy of the nomogram. Results showed that only minor differences were found between the predicted and observed overall survival, suggesting the excellent predictive accuracy of the nomogram (Figure 2(D)). In summary, high levels of inflammasome features indicated a prolonged survival in patients.

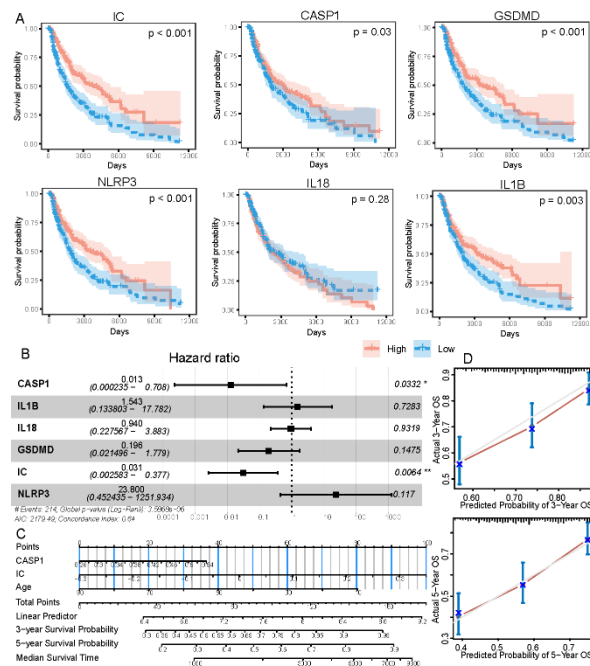


Figure 2. Association between inflammasome features and overall survival in SKCM patients. (A) The K-M curves compare the survival difference between high and low inflammasome groups. (B) The forest plot illustrates independent prognostic factors identified by the multi-variable Cox regression model. (C) The nomogram shows the prediction model constructed using independent prognostic factors. (D) The calibration curves evaluate the predictive performance of the nomogram.

3.3. The oncogenic role of inflammasome features in SKCM

Here, we calculated the overall inflammasome feature score (IM score) using ssGSEA based on all the inflammasome-related genes in the aforementioned six gene sets. All samples were divided into two subgroups according to the median value of the IM score (Figure 3(A)). K-M curves showed that patients with higher levels of an IM score presented better OS and PFS than those with lower scores (Figure 3(B)). Therefore, we sought to explore the differences between the two subgroups.

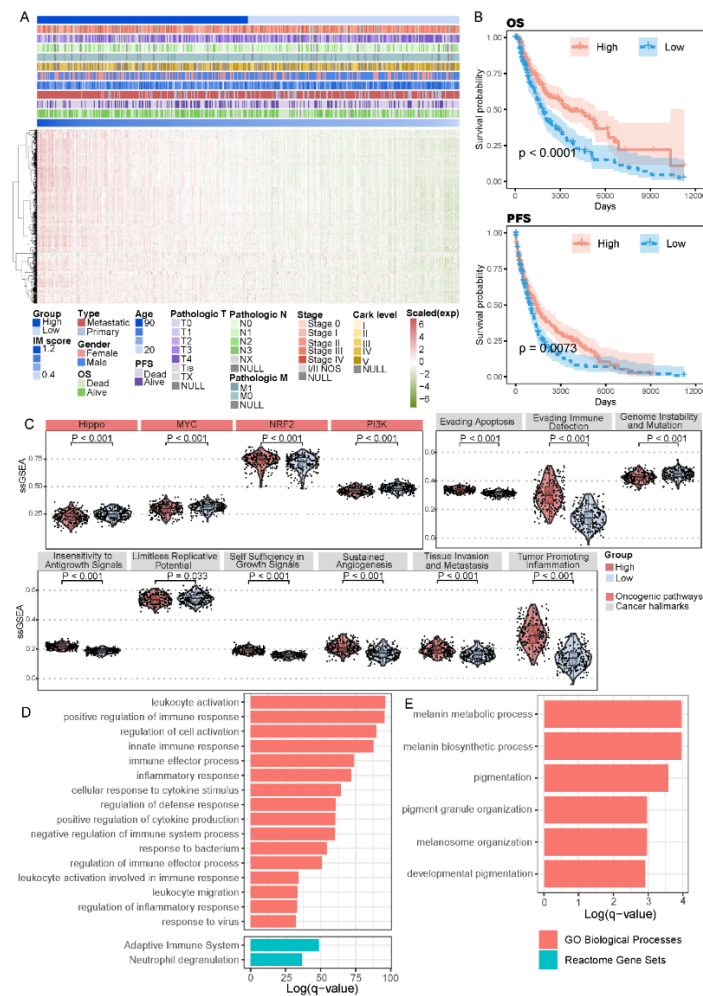


Figure 3. Oncogenic role of inflammasome features. (A) Heatmap shows the expression patterns of dysregulated genes between high and low inflammasome groups. (B) Survival differences between high and low inflammasome groups. (C) Expression levels of cancer hallmarks and oncogenic pathways in high and low inflammasome groups. (D) Functional enrichment results for up-regulated genes. (E) Functional enrichment results for down-regulated genes.

First, we quantified the enrichment level of ten oncogenic pathways and ten cancer hallmark gene sets using ssGSEA (Figure 3(C), Figure S4). As a result, the NRF2 pathway was upregulated in the high IM score subgroup, while the Hippo, MYC, and PI3K pathways were downregulated in the high IM subgroup. As for the cancer hallmark gene sets, except for Reprogramming Energy Metabolism, all hallmarks

exhibited significant expression differences between the two subgroups. The Genome Instability and Mutation and Limitless Replicative Potential gene set showed a higher level in the low IM subgroup, while other hallmarks showed an opposing pattern. Next, we performed a differential expression analysis on all protein-coding genes to further investigate the differences between the two subgroups (Figure 3(A)). As a result, 643 dysregulated genes were identified (13 downregulated and 630 upregulated genes). We performed a functional enrichment analysis on upregulated and downregulated genes. As a result, downregulated genes were enriched in melanin- and pigment-related biological processes (Figure 3(E)). The upregulated genes were associated with various immune response-related biological processes (Figure 3(D)). In conclusion, our analysis revealed the oncogenic role of inflammasome features in SKCM.

3.4. IM score was correlated with the TIME

Given the enrichment analysis result, we sought to investigate the relationship between the inflammasome features and TIME. A previous study collected 29 knowledge-based gene expression signatures to describe the functional and cellular components of TIME. Here, we quantified the enrichment level of 29 signatures using ssGSEA on SKCM samples. Then, we performed an unsupervised hierarchical clustering method on TIME signatures. As a result, four immune clusters were identified (Figure 4(A)).

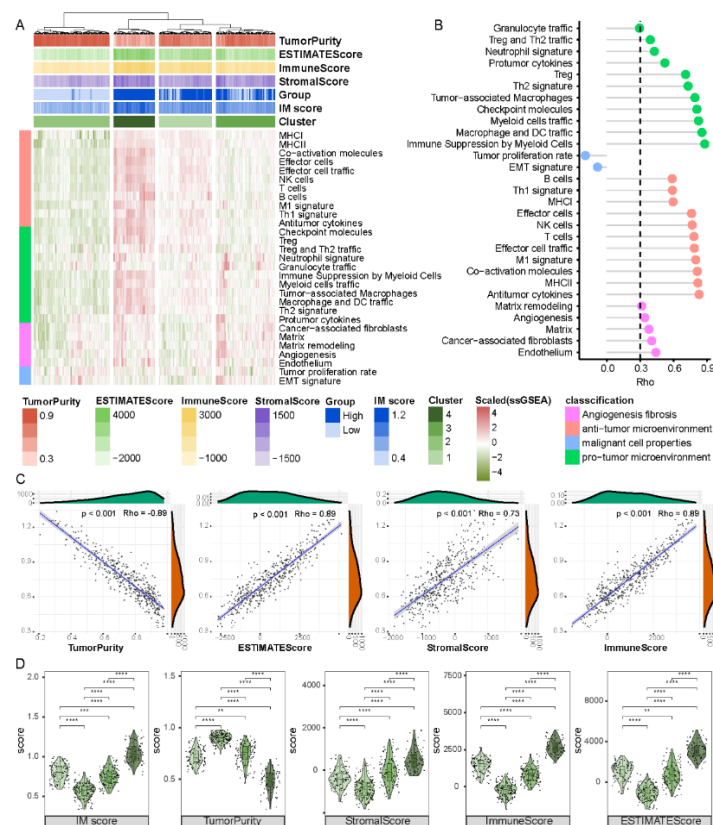


Figure 4. Associations between TIME and inflammasomes. (A) Expression patterns of 29 TIME signatures. (B) Correlations between the 29 TIME signatures and IM score. (C) Correlations between ESTIMATE-calculated TIME scores and IM score. (D) Differences in TIME scores among four immune clusters.

As shown in the figure, the IM score exhibited the highest level in cluster 4 and the lowest level in cluster 2 (Figure 4(D)). Additionally, anti- and pro-tumor microenvironment-related signatures were higher in cluster 4 compared to other clusters (Figure 4(A)). Spearman's correlation analysis showed that all TIME signatures were positively correlated with the IM score, except for EMT and tumor proliferation rate-related signatures (Figure 4(B)). However, the expression levels of all TIME signatures exhibited significant differences across four immune clusters (Figure S5). As for the ESTIMATE-generated TIME patterns, the immune, stromal, and ESTIMATE scores showed positive correlations with the IM score (Figure 4C) and exhibited the highest level in cluster 4. However, tumor purity was negatively correlated with the IM score and showed the lowest level in cluster 4 (Figure 4(D)). In summary, the different clusters defined by TIME signatures were closely associated with inflammasome features.

3.5. Identification of two inflammasome-related subtypes

Here, we applied the consensus clustering method on TCGA SKCM patients using inflammasome feature scores. Based on the Calinski criterion and the relative change in the area under the CDF curves, two SKCM subtypes were identified: subtype 1 included 313 patients (66.88%), and subtype 2 included 155 patients (33.12%) (Figure 5(A), (C) and (D)). First, a survival analysis revealed distinct survival outcomes between two subtypes: patients from subtype 2 had a better overall survival compared to those from subtype 1. Regarding PFS, subtype 2 patients only showed better survival outcomes within the 3000–6000-day interval. However, there was no significant difference in PFS across the entire time range (Figure 5(B)). Next, a sample overlap analysis suggested that immune cluster 2 was entirely classified with subtype 1, while immune cluster 4 was classified with subtype 2 (Figure 5(E) and (F)). The majority of immune cluster 3 was in subtype 1, whereas immune cluster 1 was almost evenly distributed between the two subtypes. Furthermore, subtype 1 demonstrated relatively lower levels of the IM score, while subtype 2 exhibited relatively higher levels of the IM score (Figure 5(E)). TCGA defined three melanoma subtypes [44]; here, we found that most keratin and MTF-low samples belonged to subtype 1, while most immune samples were in subtype 2 (Figure 5(F)). The results from the overlap analysis suggested potential correlations between the subtypes defined by the IM score and the SKCM immunity. In addition, we performed a differential expression analysis between two SKCM subtypes and identified 692 dysregulated genes (Figure 5(E)). Almost all dysregulated genes exhibited significantly higher expression in subtype 2 (8 upregulated genes and 684 downregulated genes in subtype 1). Lastly, we performed a GSEA enrichment on dysregulated genes between two subtypes. As a result, dysregulated genes were enriched in essential immune functions, including the immune response, cytokine-cytokine receptor interaction [45], the apoptotic process, and the T cell receptor signaling pathway [46] (Figure 5(G)). These pathways represent the core functions and crucial regulatory processes of the immune system. The results of the functional enrichment analysis further validated the correlations between the IM score-defined subtypes and the immune response of SKCM patients. This provided additional support for the notion that inflammasome features could potentially serve as predictive indicators of the patients' responses to ICB therapy.

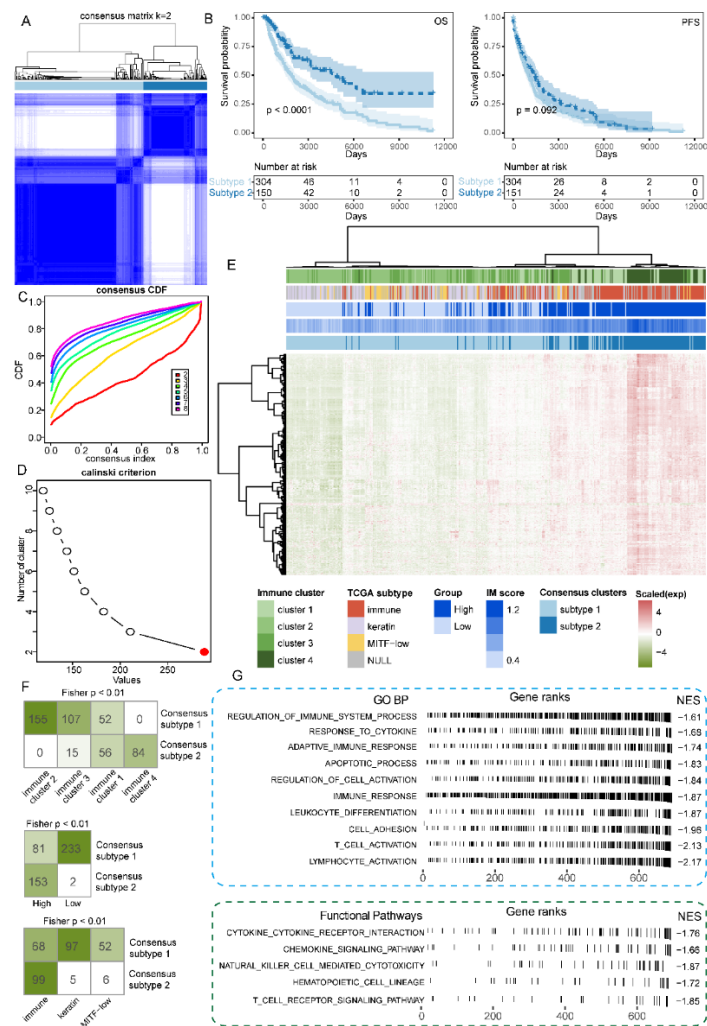


Figure 5. Identification of two inflammasome-associated subtypes. (A) Two SKCM subtypes identified by consensus clustering. (B) Survival differences between the two SKCM subtypes. (C) The relative change in the area under the CDF curve (from $k = 2$ to 8). (D) Optimal clustering k calculated by Calinski criterion. (E) Differentially expressed genes between two subtypes. (F) Overlap analysis between samples generated by different classification methods. (G) GSEA for differentially expressed genes.

3.6. Inflammasome features predicted ICB therapy response

Here, we collected three cohorts of SKCM patients who received ICB therapy (Table 1). First, we found higher expression levels of inflammasome features in responders among all three cohorts compared to non-responders (Figure 6(A), (H) and (I)). More specifically, in the Gide (anti-PD-1) cohort, the expression levels of the GSDMD, IL1B, IL18, and NLRP3 features were significantly correlated with the ICB response (Figure 6(A)). A similar pattern was found in the Gide (anti-CTLA-4 + PD-1) cohort (Figure 6(H)). Moreover, in the GSE91061 cohort, the expression level of the CASP1 feature showed significant differences between the two types of patients (Figure 6(I)).

Next, we performed a ROC analysis on the features with expression differences between responders and non-responders of the three cohorts. As a result, all four features showed high AUC values in the Gide

(anti-PD-1) cohort, with the IL18 feature achieving the highest AUC of 0.837, suggesting its excellent predictive ability (Figure 6(B)). Additionally, the IL1B, IL18, and NLRP3 features demonstrated a strong discriminatory ability among patients in the Gide (anti-PD-1 + CTLA4) cohort and the GSE91061 cohort (Figure 6(F) and (G)). Moreover, we trained an SVM classifier using the Gide (anti-PD-1) cohort to predict the ICB therapy response of TCGA SKCM patients. The expression level of inflammasome features could effectively discriminate between the predicted responders and non-responders (Figure 6(C)). As shown in the K-M curve, the predicted responders had better overall survival than the predicted non-responders (Figure 6(D)), further suggesting the predictive ability of the inflammasome features. Lastly, among the three TCGA SKCM subtypes, the immune subtype exhibited the highest possibility of response, consistent with the predicted results (Figure 6(E)). In summary, inflammasome features could predict the response to ICB therapy in SKCM patients.

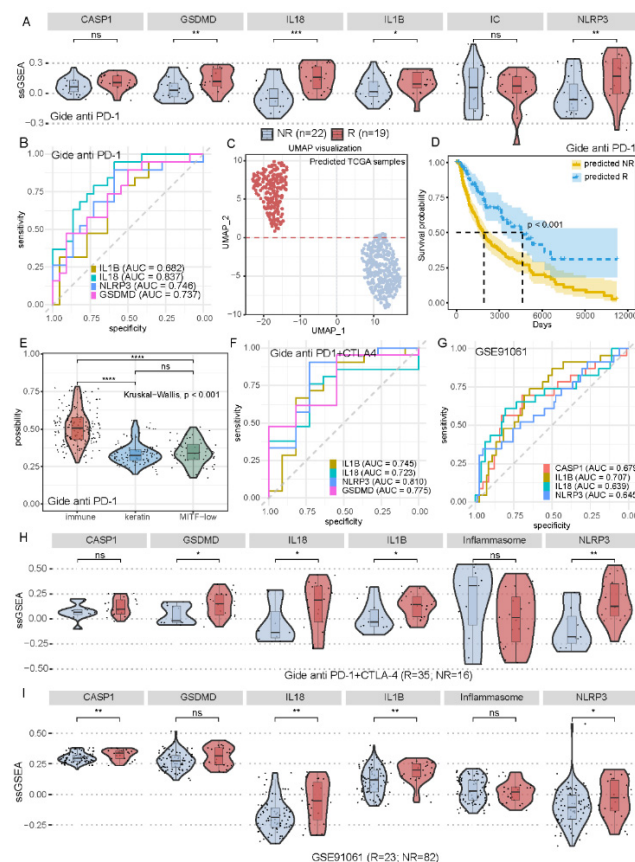


Figure 6. Prediction of ICB therapy response by inflammasome features. (A) Expression levels of inflammasome features in responders vs non-responders. (B) ROC curves corresponding to each inflammasome feature. (C) UMAP plot depicting sample dimensionality reduction using inflammasome features. (D) Differences in overall survival between predicted responders and non-responders. (E) Possibilities of response in patients across the three TCGA subtypes. (F) ROC curves corresponding to each inflammasome feature (Gide anti-CTLA-4 + PD-1 cohort). (G) ROC curves corresponding to each inflammasome feature (GSE91061). (H) Expression levels of inflammasome features in responders vs non-responders (Gide anti-CTLA-4 + PD-1 cohort). (I) Expression levels of inflammasome features in responders vs non-responders (GSE91061).

4. Conclusions

Our study provided a systematic insight into the dysregulation of the inflammasomes in aggressive SKCM. We observed elevated expression levels of inflammasome activation markers, suggesting increased inflammasome activity in SKCM. Our findings also revealed a strong correlation between inflammasome activation and the immune cell composition within the tumor microenvironment, highlighting its role in shaping the immune response in SKCM. Importantly, we found a significant association between inflammasome activation and the response to immune checkpoint blockade therapy in SKCM. Overall, our study emphasized the critical role of the inflammasomes in SKCM, from tumor development and immune microenvironment modulation to therapeutic response.

5. Discussion

SKCM is one of the most aggressive forms of skin cancer, characterized by its high metastatic potential and resistance to conventional therapies [1,2]. The emerging link between inflammation and SKCM has gained significant attention [47], with previous studies demonstrating the involvement of inflammatory processes in the progression and metastasis of SKCM [48]. The inflammasome, which is a vital complex composed of multiple proteins, exerts its role during inflammatory immune reactions [49]. The inflammasome detects pathogens and triggers inflammatory responses. The coordinated actions in inflammasome signaling collectively contribute to regulating inflammation and the immune response mediated by the inflammasome.

In this study, we comprehensively investigated the expression patterns of the inflammasome features and their correlations with clinical characteristics in SKCM patients, revealing significant dysregulation of the inflammasome in SKCM. Specifically, we observed elevated expression levels of CASP1 and NLRP3, which are responsible for inflammasome activation, suggesting increased inflammasome activity in SKCM (Figure 1(A)). Additionally, we found that the expression level of GSDMD, which is a downstream effector of inflammasome activation, was lower than other features, indicating a potential disruption of pyroptosis in SKCM. These findings highlighted the perturbation of inflammasome components in SKCM and provided insights into the potential involvement of the inflammasome in the pathogenesis and progression of this aggressive skin cancer. In addition, we observed a decrease in the expression of IL-1 β and IL-18 in the cancer samples, indicating a potential disruption of their pro-inflammatory functions in SKCM [29]. The decreased expression of IL-1 β and IL-18 suggests a potential impairment in the activation of downstream inflammatory signaling pathways, which could impact immune responses and contribute to the tumor microenvironment's immune evasion mechanisms. It is worth noting that in Result 4, we found various correlations between inflammasome features and TIME signatures. Future studies should investigate the impact of TIME components disturbances in the inflammasome.

The inflammasome has been shown to play a crucial role in shaping the tumor microenvironment by modulating the immune response [29]. Activation of the inflammasome can induce programmed cell death in cancer cells and inhibit tumor growth. Dysregulation of the inflammasome has been associated with developing immune escape mechanisms, leading to tumor progression and poor clinical outcomes [25]. In this study, we employed the TIME signature derived from a previous study [35] to perform unsupervised clustering of SKCM patients. We investigated the association between immune

clusters and inflammasome feature scores. The results revealed that immune cluster 4 exhibited the highest inflammasome feature scores and TIME signature levels. This finding suggested a strong correlation between the activation of the inflammasome and the immune cell composition within immune cluster 4, as indicated by the TIME signature (Figure 4(A)). These results provided valuable insights into the potential role of inflammasome activation in shaping the immune microenvironment of SKCM. They highlighted the importance of further investigating the functional implications of this association. The identification of two IM score-defined subtypes further proved the association between the inflammasome and SKCM immunity, as the results showed significant overlaps between IM subtypes and distinct SKCM immune clusters. Collectively, these results implied the potential of using inflammasome features to predict the patients' ICB therapy response.

Immunotherapy, particularly ICB, has emerged as a promising treatment approach for SKCM [50]; however, only a limited number of patients benefit from the treatment [43,51,52]. There is growing evidence suggesting a significant association between inflammasome activation and the response to ICB therapy in SKCM [53], highlighting the potential of targeting inflammasome pathways to enhance the efficacy of immunotherapy [54]. Our study revealed a close association between the inflammasome and immune function in SKCM (Figures 4 and 5). Consequently, we further explored the correlation between the inflammasome and the patients' response to ICB therapy. In the ICB cohorts, we identified significant upregulation of inflammasome expression in responders. This finding suggested that inflammasome activation may play a crucial role in enhancing the efficacy of ICB by promoting immune activation [55]. Furthermore, the increased expression of the inflammasome in responders highlights the potential of targeting inflammasome components as a promising strategy to enhance the clinical benefits of immunotherapy in SKCM patients. In conclusion, our study revealed the significant association of dysregulated inflammasome expression with tumor development, the immune microenvironment, and immune therapy response in SKCM. These findings underscored the critical role of the inflammasome in SKCM. Additionally, they lay the foundation for developing potential therapeutic strategies and prognostic markers in SKCM.

Use of AI tools declaration

The authors declare they have not used Artificial Intelligence (AI) tools in the creation of this article.

Acknowledgments

This work was supported by the Natural Science Fund of Heilongjiang Province [LH2020H038], and Research and Innovation Fund of the First Affiliated Hospital of Harbin Medical University [2019M12].

Conflict of interest

The authors declare there is no conflict of interest.

References

1. D. Schadendorf, D. E. Fisher, C. Garbe, J. E. Gershenwald, J. Grob, A. Halpern, et al., Melanoma, *Nat. Rev. Dis. Primers*, **1** (2015), 15003. <https://doi.org/10.1038/nrdp.2015.3>
2. A. M. M. Eggermont, A. Spatz, C. Robert, Cutaneous melanoma, *Lancet*, **383** (2014), 816–827. [https://doi.org/10.1016/S0140-6736\(13\)60802-8](https://doi.org/10.1016/S0140-6736(13)60802-8)
3. G. C. Leonardi, L. Falzone, R. Salemi, A. Zanghi, D. A. Spandidos, J. A. McCubrey, et al., Cutaneous melanoma: From pathogenesis to therapy (Review), *Int. J. Oncol.*, **52** (2018), 1071–1080. <https://doi.org/10.3892/ijo.2018.4287>
4. D. J. Shah, R. S. Dronca, Latest advances in chemotherapeutic, targeted, and immune approaches in the treatment of metastatic melanoma, *Mayo Clin. Proc.*, **89** (2014), 504–519. <https://doi.org/10.1016/j.mayocp.2014.02.002>
5. P. P. Centeno, V. Pavet, R. Marais, The journey from melanocytes to melanoma, *Nat. Rev. Cancer*, **23** (2023), 372–390. <https://doi.org/10.1038/s41568-023-00565-7>
6. F. R. Greten, S. I. Grivennikov, Inflammation and cancer: Triggers, mechanisms, and consequences, *Immunity*, **51** (2019), 27–41. <https://doi.org/10.1016/j.immuni.2019.06.025>
7. J. Amin, D. Boche, S. Rakic, What do we know about the inflammasome in humans?, *Brain Pathol.*, **27** (2017), 192–204. <https://doi.org/10.1111/bpa.12479>
8. F. Martinon, K. Burns, J. Tschopp, The inflammasome: a molecular platform triggering activation of inflammatory caspases and processing of proIL-beta, *Mol. Cell*, **10** (2002), 417–426. [https://doi.org/10.1016/s1097-2765\(02\)00599-3](https://doi.org/10.1016/s1097-2765(02)00599-3)
9. T. Strowig, J. Henao-Mejia, E. Elinav, R. Flavell, Inflammasomes in health and disease, *Nature*, **481** (2012), 278–286. <https://doi.org/10.1038/nature10759>
10. R. Karki, S. M. Man, T. Kanneganti, Inflammasomes and Cancer, *Cancer Immunol. Res.*, **5** (2017), 94–99. <https://doi.org/10.1158/2326-6066.CIR-16-0269>
11. V. A. K. Rathinam, S. K. Vanaja, K. A. Fitzgerald, Regulation of inflammasome signaling, *Nat. Immunol.*, **13** (2012), 333–342. <https://doi.org/10.1038/ni.2237>
12. N. Kayagaki, I. B. Stowe, B. L. Lee, K. O'Rourke, K. Anderson, S. Warming, et al., Caspase-11 cleaves gasdermin D for non-canonical inflammasome signalling, *Nature*, **526** (2015), 666–671. <https://doi.org/10.1038/nature15541>
13. J. Shi, Y. Zhao, K. Wang, X. Shi, Y. Wang, H. Huang, et al., Cleavage of GSDMD by inflammatory caspases determines pyroptotic cell death, *Nature*, **526** (2015), 660–665. <https://doi.org/10.1038/nature15514>
14. Y. Li, G. Nanayakkara, Y. Sun, X. Li, L. Wang, R. Cueto, et al., Analyses of caspase-1-regulated transcriptomes in various tissues lead to identification of novel IL-1 β -, IL-18- and sirtuin-1-independent pathways, *J. Hematol. Oncol.*, **10** (2017), 40. <https://doi.org/10.1186/s13045-017-0406-2>
15. C. Jin, R. A. Flavell, Molecular mechanism of NLRP3 inflammasome activation, *J. Clin. Immunol.*, **30** (2010), 628–631. <https://doi.org/10.1007/s10875-010-9440-3>
16. L. Chen, L. Wang, N. Tsang, D. M. Ojcius, C. Chen, C. Ouyang, et al., Tumour inflammasome-derived IL-1 β recruits neutrophils and improves local recurrence-free survival in EBV-induced nasopharyngeal carcinoma, *EMBO Mol. Med.*, **4** (2012), 1276–1293. <https://doi.org/10.1002/emmm.201201569>
17. M. S. Carlino, J. Larkin, G. V. Long, Immune checkpoint inhibitors in melanoma, *Lancet*, **398** (2021), 1002–1014. [https://doi.org/10.1016/S0140-6736\(21\)01206-X](https://doi.org/10.1016/S0140-6736(21)01206-X)

18. D. M. Pardoll, The blockade of immune checkpoints in cancer immunotherapy, *Nat. Rev. Cancer*, **12** (2012), 252–264. <https://doi.org/10.1038/nrc3239>
19. M. A. Curran, W. Montalvo, H. Yagita, J. P. Allison, PD-1 and CTLA-4 combination blockade expands infiltrating T cells and reduces regulatory T and myeloid cells within B16 melanoma tumors, *Proc. Natl. Acad. Sci.*, **107** (2010), 4275–4280. <https://doi.org/10.1073/pnas.0915174107>
20. E. M. Van Allen, D. Miao, B. Schilling, S. A. Shukla, C. Blank, L. Zimmer, et al., Genomic correlates of response to CTLA-4 blockade in metastatic melanoma, *Science*, **350** (2015), 207–211. <https://doi.org/10.1126/science.aad0095>
21. C. N. Owen, X. Bai, T. Quah, S. N. Lo, C. Allayous, S. Callaghan, et al., Delayed immune-related adverse events with anti-PD-1-based immunotherapy in melanoma, *Ann. Oncol.*, **32** (2021), 917–925. <https://doi.org/10.1016/j.annonc.2021.03.204>
22. J. Larkin, V. Chiarion-Sileni, R. Gonzalez, J. Grob, P. Rutkowski, C. D. Lao, et al., Five-year survival with combined nivolumab and ipilimumab in advanced melanoma, *New Engl. J. Med.*, **381** (2019), 1535–1546. <https://doi.org/10.1056/NEJMoa1910836>
23. J. Larkin, C. D. Lao, W. J. Urba, D. F. McDermott, C. Horak, J. Jiang, et al., Efficacy and safety of nivolumab in patients with braf v600 mutant and braf wild-type advanced melanoma: A pooled analysis of 4 clinical trials, *JAMA Oncol.*, **1** (2015), 433–440. <https://doi.org/10.1001/jamaoncol.2015.1184>
24. J. Larkin, V. Chiarion-Sileni, R. Gonzalez, J. J. Grob, C. L. Cowey, C. D. Lao, et al., Combined nivolumab and ipilimumab or monotherapy in untreated melanoma, *New Engl. J. Med.*, **373** (2015), 23–34. <https://doi.org/10.1056/NEJMoa1504030>
25. J. Hou, M. Karin, B. Sun, Targeting cancer-promoting inflammation - have anti-inflammatory therapies come of age?, *Nat. Rev. Clin. Oncol.*, **18** (2021), 261–279. <https://doi.org/10.1038/s41571-020-00459-9>
26. B. Theivanthiran, K. S. Evans, N. C. DeVito, M. Plebanek, M. Sturdivant, L. P. Wachsmuth, et al., A tumor-intrinsic PD-L1/NLRP3 inflammasome signaling pathway drives resistance to anti-PD-1 immunotherapy, *J. Clin. Invest.*, **130** (2020), 2570–2586. <https://doi.org/10.1172/JCI133055>
27. C. I. Diakos, K. A. Charles, D. C. McMillan, S. J. Clarke, Cancer-related inflammation and treatment effectiveness, *Lancet Oncol.*, **15** (2014), 493–503. [https://doi.org/10.1016/S1470-2045\(14\)70263-3](https://doi.org/10.1016/S1470-2045(14)70263-3)
28. M. Ju, J. Bi, Q. Wei, L. Jiang, Q. Guan, M. Zhang, et al., Pan-cancer analysis of NLRP3 inflammasome with potential implications in prognosis and immunotherapy in human cancer, *Briefings Bioinf.*, **22** (2021), 345. <https://doi.org/10.1093/bib/bbaa345>
29. R. Karki, T. Kanneganti, Diverging inflammasome signals in tumorigenesis and potential targeting, *Nat. Rev. Cancer*, **19** (2019), 197–214. <https://doi.org/10.1038/s41568-019-0123-y>
30. Q. Liang, J. Wu, X. Zhao, S. Shen, C. Zhu, T. Liu, et al., Establishment of tumor inflammasome clusters with distinct immunogenomic landscape aids immunotherapy, *Theranostics*, **11** (2021), 9884–9903. <https://doi.org/10.7150/thno.63202>
31. J. Lonsdale, J. Thomas, M. Salvatore, R. Phillips, E. Lo, S. Shad, et al., The Genotype-Tissue Expression (GTEx) project, *Nat. Genet.*, **45** (2013), 580–585. <https://doi.org/10.1038/ng.2653>
32. M. J. Goldman, B. Craft, M. Hastie, K. Repecka, F. McDade, A. Kamath, et al., Visualizing and interpreting cancer genomics data via the Xena platform, *Nat. Biotechnol.*, **38** (2020), 675–678. <https://doi.org/10.1038/s41587-020-0546-8>
33. M. E. Ritchie, B. Phipson, D. Wu, Y. Hu, C. W. Law, W. Shi, et al., limma powers differential expression analyses for RNA-sequencing and microarray studies, *Nucleic Acids Res.*, **43** (2015), 47. <https://doi.org/10.1093/nar/gkv007>

34. K. Yoshihara, M. Shahmoradgoli, E. Martinez, R. Vegesna, H. Kim, W. Torres-Garcia, et al., Inferring tumour purity and stromal and immune cell admixture from expression data, *Nat. Commun.*, **4** (2013), 2612. <https://doi.org/10.1038/ncomms3612>
35. A. Bagaev, N. Kotlov, K. Nomie, V. Svelkolkin, A. Gafurov, O. Isaeva, et al., Conserved pan-cancer microenvironment subtypes predict response to immunotherapy, *Cancer Cell*, **39** (2021), 845–865. <https://doi.org/10.1016/j.ccell.2021.04.014>
36. M. D. Wilkerson, D. N. Hayes, ConsensusClusterPlus: a class discovery tool with confidence assessments and item tracking, *Bioinformatics*, **26** (2010), 1572–1573. <https://doi.org/10.1093/bioinformatics/btq170>
37. Y. Zhou, B. Zhou, L. Pache, M. Chang, A. H. Khodabakhshi, O. Tanaseichuk, et al., Metascape provides a biologist-oriented resource for the analysis of systems-level datasets, *Nat. Commun.*, **10** (2019), 1523. <https://doi.org/10.1038/s41467-019-09234-6>
38. F. Sanchez-Vega, M. Mina, J. Armenia, W. K. Chatila, A. Luna, K. C. La, et al., Oncogenic signaling pathways in the cancer genome atlas, *Cell*, **173** (2018), 321–337. <https://doi.org/10.1016/j.cell.2018.03.035>
39. D. Hanahan, R. A. Weinberg, Hallmarks of cancer: the next generation, *Cell*, **144** (2011), 646–674. <https://doi.org/10.1016/j.cell.2011.02.013>
40. A. Liberzon, C. Birger, H. Thorvaldsdottir, M. Ghandi, J. P. Mesirov, P. Tamayo, The Molecular Signatures Database (MSigDB) hallmark gene set collection, *Cell Syst.*, **1** (2015), 417–425. <https://doi.org/10.1016/j.cels.2015.12.004>
41. S. Hanzelmann, R. Castelo, J. Guinney, GSEA: gene set variation analysis for microarray and RNA-seq data, *BMC Bioinf.*, **14** (2013), 7. <https://doi.org/10.1186/1471-2105-14-7>
42. T. N. Gide, C. Quek, A. M. Menzies, A. T. Tasker, P. Shang, J. Holst, et al., Distinct immune cell populations define response to Anti-PD-1 monotherapy and Anti-PD-1/Anti-CTLA-4 combined therapy, *Cancer Cell*, **35** (2019), 238–255. <https://doi.org/10.1016/j.ccell.2019.01.003>
43. T. N. Gide, J. S. Wilmott, R. A. Scolyer, G. V. Long, Primary and acquired resistance to immune checkpoint inhibitors in metastatic melanoma, *Clin. Cancer Res.*, **24** (2018), 1260–1270. <https://doi.org/10.1158/1078-0432.CCR-17-2267>
44. R. Akbani, K. C. Akdemir, B. A. Aksoy, M. Albert, A. Ally, S. B. Amin, et al., Genomic classification of cutaneous melanoma, *Cell*, **161** (2015), 1681–1696. <https://doi.org/10.1016/j.cell.2015.05.044>
45. T. A. Waldmann, Cytokines in Cancer Immunotherapy, *Cold Spring Harbor Perspect. Biol.*, **10** (2018). <https://doi.org/10.1101/cshperspect.a028472>
46. M. Shakiba, P. Zumbo, G. Espinosa-Carrasco, L. Menocal, F. Dünder, S. E. Carson, et al., TCR signal strength defines distinct mechanisms of T cell dysfunction and cancer evasion, *J. Exp. Med.*, **219** (2022). <https://doi.org/10.1084/jem.20201966>
47. R. Kolb, G. Liu, A. M. Janowski, F. S. Sutterwala, W. Zhang, Inflammasomes in cancer: a double-edged sword, *Protein Cell*, **5** (2014), 12–20. <https://doi.org/10.1007/s13238-013-0001-4>
48. M. Okamoto, W. Liu, Y. Luo, A. Tanaka, X. Cai, D. A. Norris, et al., Constitutively active inflammasome in human melanoma cells mediating autoinflammation via caspase-1 processing and secretion of interleukin-1 β , *J. Biol. Chem.*, **285** (2010), 6477–6488. <https://doi.org/10.1074/jbc.M109.064907>
49. V. A. Rathinam, K. A. Fitzgerald, Inflammasome complexes: Emerging mechanisms and effector functions, *Cell*, **165** (2016), 792–800. <https://doi.org/10.1016/j.cell.2016.03.046>
50. J. M. Redman, G. T. Gibney, M. B. Atkins, Advances in immunotherapy for melanoma, *BMC Med.*, **14** (2016). <https://doi.org/10.1186/s12916-016-0571-0>

51. B. J. Schneider, J. Naidoo, B. D. Santomasso, C. Lacchetti, S. Adkins, M. Anadkat, et al., Management of immune-related adverse events in patients treated with immune checkpoint inhibitor therapy: Asco guideline update, *J. Clin. Oncol.*, **39** (2021), 4073–4126. <https://doi.org/10.1200/JCO.21.01440>
52. D. B. Johnson, C. A. Nebhan, J. J. Moslehi, J. M. Balko, Immune-checkpoint inhibitors: long-term implications of toxicity, *Nat. Rev. Clin. Oncol.*, **19** (2022), 254–267. <https://doi.org/10.1038/s41571-022-00600-w>
53. B. Theivanthiran, N. Yarla, T. Haykal, Y. V. Nguyen, L. Cao, M. Ferreira, et al., Tumor-intrinsic NLRP3-HSP70-TLR4 axis drives premetastatic niche development and hyperprogression during anti-PD-1 immunotherapy, *Sci. Transl. Med.*, **14** (2022), 7019. <https://doi.org/10.1126/scitranslmed.abq7019>
54. J. J. Havel, D. Chowell, T. A. Chan, The evolving landscape of biomarkers for checkpoint inhibitor immunotherapy, *Nat. Rev. Cancer*, **19** (2019), 133-150. <https://doi.org/10.1038/s41568-019-0116-x>
55. G. Dranoff, Cytokines in cancer pathogenesis and cancer therapy, *Nat. Rev. Cancer*, **4** (2004), 11–22. <https://doi.org/10.1038/nrc1252>



AIMS Press

©2023 the Author(s), licensee AIMS Press. This is an open access article distributed under the terms of the Creative Commons Attribution License (<http://creativecommons.org/licenses/by/4.0>)